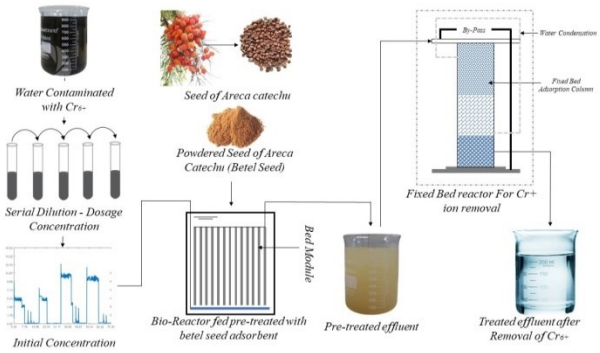
Global NEST Journal, Vol 25, No 7, pp 25-31
Copyright© 2023 Global NEST
Printed in Greece. All rights reserved

An experimental study on continuous removal of chromium (VI^+) ions from wastewater effluent by using fluidized bed reactor

Srinivasan K.[1*], Priya V.[2*], Sashik Kumar M.C. [3] and Suriya S.[4]
[1]Department of Civil Engineering, PSNA College of Engineering and Technology, Dindigul 624622, Tamilnadu, India
[2]Department of Civil Engineering, GMR Institute of Technology, Razam−632127, Andhra Pradesh, India
[3]Department of Civil Engineering, University College of Engineering, Dindigul−624622, Tamilnadu, India
[4]Department of Civil Engineering, Mepco Schlenk Engineering College, Sivakasi−626005, Tamilnadu
Received: 19/05/2023, Accepted: 24/06/2023, Available online: 30/06/2023
*to whom all correspondence should be addressed: e-mail: cksapc@gmail.com, vrpriyaashree@gmail.com
https://doi.org/10.30955/gnj.005148

Graphical abstract



Abstract

Hazardous metal chromium is used extensively in many different industrial processes and is commonly found in industrial effluents. Hazardous pollutants such inorganic anions, metal ions, synthetic xenobiotics, and others have contaminated ground and surface waters in India and other parts of the world as a result of continued industrial expansion and agricultural development. This study uses betel seed powder and a fixed bed reactor (FBR) technology running at room temperature to extract chromium (VI+) from a synthetic water environment. The fixed-bed research included significant experiments such as the development of breakthrough curves (including the effects of starting Cr (VI+) concentration, BSF size, and flow rate) and bed-depth service time (BDST) approach. Betel Seed Powder was used as a biosorbent to remove Cr (VI+) from aqueous solution. The effects of several variables, including bed height (2.5, 5.5, and 7.5 cm), flow rate of 40, 60, and 100 ml/min, were investigated at an influent pH of 6.5. It was shown that as bed depth, flow velocity, and starting concentration rose, so did the exhaustion time. The biosorptive capacity of betel seed powder in fixed bed reactor tests was approximately 8–9 times higher than that of betel seed powder in continuous stirred batch reactor study. For the removal of Cr (VI+) by BSF, the BDST method achieved a higher bed efficiency of 98.9% and was ideal. The biosorptive ability of BSP was found to be highly correlated with the initial Cr (VI+) concentration (No = 0.089Co).

Keywords: Chromium (VI^+), betel seed powder, column bed study, service time in bed, biosorption volume

1. Introduction

The modelling results demonstrated that the film-diffusion based model was adequate for fitting the lab-scale data as well as for modelling the large-lab breakthrough curves of Cr (VI) elimination using both uncoated and coated biomass. In recent years, many biological and physiochemical methods have been utilised to remove Cr (VI+) from water, including reverse osmosis, ion exchange, electrodialysis, and others. Because of the slower reduction rate, complicated methods, and expensive alleged operations, researchers were still keen to discover a solution. Heavy metals in wastewater still constitute a significant difficulty for selecting the optimal technology for treating industrial and urban effluents in wastewater treatment plants. Hexavalent chromium, Cr (VI), is a very dangerous chemical due to its high solubility, mobility, and oxidation potential as well as its bioavailability. It finds heavy metals and offers information on their content and level of toxicity in the water Environmental pollution caused by both organised and unstructured industrial expansion, poor effluent treatment due to ignorance and subpar treatment facilities, and environmental contamination pose a serious threat to global health today (Gokulan R. *et al*., 2022). Chromium (VI) is ranked 16th on the Agency for Toxic Substances and Disease Registry's priority list (ATSDR) (Zhike Wang Cunling *et al*., 2013).

Fixed bed reactors have substantially higher heat exchange efficiency than fixed beds and better temperature control due to turbulent gas flow and quick circulation. Despite being widely used across a wide range of sectors, traditional fluidized beds have a number of disadvantages (Blanco C *et al*., 2021). Slugging, bubbling, elutriation, and channelling have a major detrimental

effect on the effectiveness and quality of large and deep gas-solid fluidized beds when gas velocities are higher than the minimum fluidization velocity. Fluidized bed reactors offer a much higher efficiency in heat exchange, compared to fixed beds, and better temperature control, due to the turbulent gas flow and rapid circulation. The removal efficiency of Chromium ions increases, while treating the effluent with adsorbent like betal seeds etc One of these physical methods, adsorption, is mainly employed to remediate wastewater. Matching the activated carbon or charcoal's pore size to the size of the gas molecule you want to adsorb is the first step in increasing efficiency. More so than pore size or adsorption efficiency, the choice between a powder and granular product relies on the application or usage (such as batch vs column mode). Granular and powder kinetics, however, will be very different, with powdered carbon having far better kinetics than granular. Granular activated carbon, on the other hand, may frequently be regenerate whereas powdered activated carbon cannot. Matching the carbon pore size to the size of the gas molecule you want to adsorb is the first step in increasing efficiency.

Simple, affordable, and ecologically responsible is biosorption. Numerous adsorbents, such as activated carbon, chitosan, polymeric resins, and other clay-based adsorbents, are used for the adsorption of organic pollutants (Gokulan R *et al*, 2021). One that can be made at low temperatures (600 °C) is the low-cost adsorbent. Mass yield falls as production temperature rises, and mass efficiency values in the range of 50% are recommended. Larger values are not very important because a specific surface on the order of 600 m^2/g will be sufficient. The same holds true for active carbon. Furthermore, if the raw material is free (as is the case with food waste), the cost price may be greatly decreased Each strategy has benefits and drawbacks. For instance, membrane filtration is thought to be relatively costly but also highly effective in removing heavy metal ions without the need for additional room. Although coagulation is said to be a cheap process, it uses a lot of chemicals. Because it is so easy to use, adsorption is thought to be one of the most practical and efficient ways to remove pollutants from wastewater effluents.

Details about the pollutants, treatments, applications, and processes are taken into account. One of the heavy metals with practical applications is chromium (VI+), which is utilised in the production of stainless steel, metallurgy, the creation of batteries and super alloys, and electroplating (Sharma Mona *et al*., 2011). In other words, as the depth of the reactor grows, so does the removal efficiency of the heavy metal concentration, or vice versa. The depth parameters are directly related to the removal efficiency of the impurities in the reactor. While the effluent is being treated with an adsorbent, the effectiveness of heavy metal removal rises. Using a dynamic technique that would enable industrial-scale treatment, column biosorption experiments were carried out to enhance the generation of cleaner effluents and to better understand the fundamental processes involved in the removal process (Vivek Sivakumar *et al*., 2022). When compared to efficiency without the pretreatment, the reactor's efficiency rises by 28.1%.

The theoretical breakthrough curve generation, the bed-depth service time (BDST) approach, the empty bed contact time (EBCT) model implementation, the assessment of movement mass-transfer zone (MTZ) through multiple ports in FBR, and the generation of breakthrough curves were all a part of the fixed-bed studies. By modifying the cuts and gradients throughout the height of the column, the geometry is changed to enhance flow rate (speed). Recent research have optimised bed height.

2. Materials and methods

2.1. Biosorbent

Areca Catechu, often known as betel seed from a far-off field, betel seeds are harvested, dried, and then powdered after the seed coat has been removed. These powdered seeds are cleaned to eliminate any impurities before being sieved to a certain size. Future studies will employ the purified seed powder, which is kept in an airtight container as the biosorbents. After being repeatedly washed in clean water to remove debris and dust, the betel seeds were collected and air-dried for seven days. The sample, which had previously been air-dried, was subsequently dried in an oven at 75 °C for 24 hours to prevent cell denaturing (Selvakumar *et al*., 2022). The oven-dried sample was ground to a fine powder using a grinding machine. It was sieved through many sieves with mesh sizes ranging from 95 to 450 m to get microscopic particles, and it was then put in desiccators for subsequent usage (Chan *et al*., 1991). Without the requirement for extra chemical processing, Cr (VI+) was removed using this material (Bhattacharya *et al*., 2019). The physiochemical properties of betel seeds are displayed in Table 1.

Table 1. Physiochemical characteristics of betel seeds

S.No.	Parameter	Result	References
1	pH range	3.12	APHA(2005)-4500
2	Weight loss after washing with 1 litre of distilled water	3 %	APHA (2005) – 5220B
3	Bulk density, kg/m^3	0.49-0.55	Ravidaran et. al., 2022
4	Moisture content	60 %	APHA (2005) – 2540F
5	Specific gravity	1.27	APHA (2005) – 2710 D
6	Nitrogen	2.4-7.1 %	Chan et. al., 1991
7	Porosity	0.21-0.36 %	Lowry's method
8	Phosphorus	0.04-0.007 %	Anthrone method

2.2. Reagents

A stock solution with a concentration of 1000 mg/L Cr (VI) was made by dissolving 2.82 g of $K_2Cr_2O_7$ in 1000 mL of double-distilled water. To get the required concentrations, the stock standard solution was sequentially diluted. All of the aqueous solutions were created using double-distilled water. The Cr (VI) content was examined in distilled water (Dabrowski *et al*., 2004). The distilled water was found to have an electrical conductivity of 2.76 S/cm, an average pH of 6.54, and a density of 981 kg/m_3. The initial pH was modified using 0.1 M soda (NaOH) and Hydrochloric acid (HCl) solutions.

2.3. Study of Cr (VI+)

Diphenylcarbazide, a complicated compound, and an excellent quartz cuvette with a route length of 10 mm and a maximum wavelength of 540 nm were utilised in the experiment. A spectrophotometric calculation was made to determine the amount of residual chromium (VI+) ions present in the effluent. It is feasible to measure the concentration of chromium (VI+) in water using spectrophotometry, Diphenylcarbazide as the reagent, and a maximum wavelength of 540 nm at pH 1 (Thangavelu *et al*., 2022). All organic material was destroyed by acid digestion, and biological and organic materials were removed; only the remaining inorganic material needed to be taken into account for potential interference. The results of the experiment showed that Cr could be detected using 0.0015% Diphenylcarbazide (VI+). According to all of the research, the experimental error was determined to be between 3 and 5% (Forstner *et al*., 1979). Using soil samples that have undergone an H_2O_2-treatment, desorption studies are also conducted to determine how organic matter affects desorption. It has been demonstrated that reducing organic matter considerably increases the amount of desorption (Ravidaran *et al*., 2022).

2.4. Column studies

On a column, hexavalent chromium biosorption tests were carried out at ideal pH 2.5, bed height, flow velocity, and initial chromium concentration (Rengaraj *et al*., 2001). Calculating the breakthrough time requires the breakthrough curve to be present. To compute the breakthrough time, the breakthrough curve must be determined. We may do this by running a column with an arbitrary diameter and length and then calculating the actual capacity and length of the equilibrium section. The diameter and length can be recalculated using these parameters. In order to do this, we can run a column with any diameter and length to determine the real capacity and length of the equilibrium section. The diameter and length may be recalculated using those factors. The glass fixed-bed column was 20 cm tall with an inside diameter of 1 cm. Using different starting adsorbent concentrations (10, 20, 40, and 60 mg/l) and sorbent bed heights (6, 12, and 18 cm, respectively), column research was conducted at 30°C and pH 2.5. The flow rate through the column was set at 50, 80, or 100 mL/min. Effluent samples were regularly collected to determine the level of hexavalent chromium in the solutions (Manoj *et al*., 2022). The level of concentration changes with time in a fixed-bed column investigation. Fixed-bed studies are used to determine the bed biosorption capacity, which is distinct from the biosorption capacity determined by batch experiments and isotherm plots. The starting doses are often determined by doing batch tests. In some circumstances, the concentration of the raw effluents will be taken into account when determining the ideal value.

The flow in the fixed-bed column was continuously maintained after the concentration of hexavalent chromium in the effluent and influent reached parity (Sapna *et al*., 2022). The separation characteristics are significantly influenced by particle size. As the diameter of the column is decreased or as the height of the bed is raised, the minimum flow velocity rises. These patterns demonstrate how wall size affects bed height and flow rate. The heavy metal content of the solution is relatively secondary data except for determining the overall concentration that can be mobilized.

The effectiveness of the biosorption process dictates how quickly the process moves forward. Biosorption capacity is proportional to the concentration of adsorbate on the adsorbate surface. The more effective an adsorbent is in removing pollutants, the higher its biosorption capacity (measured in mg/g or mmol/g). The adsorption isotherm's form represents the affinity of the adsorbate for the adsorbent and sheds light on potential interactional mechanisms. Both of the observed isotherms fall into the category of L curves for liquid-solid adsorption systems. To establish the best biosorption conditions mathematically, the breakthrough curve of each metal must be determined in order to analyse the system's operation and dynamic reaction.

2.5. Analytical techniques

A colorimetric method was used to ascertain the samples' Cr (VI) content. The pink complex formed at 540 nm by 1,5-diphenycarbazide and Cr (VI) was measured using a UV-visible spectrophotometer. It finds heavy metals and gives information on their content and toxicity in the water. controlling the feed temperature and the column bed temperature using small-scale columns and water baths. To regulate the temperature, heating tapes with a regulator can also be wrapped around the column.

2.6. Column data analysis

The fixed-bed column's effectiveness was shown by the breakthrough curves. A breakthrough's development period and the shape of the breakthrough curve play key roles in determining how well a sorption column functions and how it responds dynamically. Alkaline or acidic environment as well as temperature has the most important role in enhancing the sorption capacity of heavy metals. An essential component of the entire adsorption process is the adsorbent's point of zero charges (pzc). The surface charge is related to the zeta potential rather than the zero-point charge. If the zeta

potential is negative, the surface charge is positive, and vice versa. Because it enables you to alter the total surface charge density of the adsorbents opposite to that of the adsorbate, pH maintenance is essential to getting the maximum adsorption rate. The effluent concentration (Ct) from the column that reaches around 0.1% of the influent concentration (C0) is the breakthrough concentration. The shape of the sorption isotherm describes the affinity of the sorbate towards the adsorbent and provides insight into the possible mechanism of interaction. Both isotherms observed can be classified as L curves according to the classification for liquid-solid adsorption systems. When the effluent concentration hits 95%, that is when the "point of column exhaustion" occurs. For a certain bed depth, the breakthrough curve is often represented as Ct/C0 as a function of time or effluent volume. Running the column with illogical values will provide a general notion of how to set the parameters. The length and diameter of the fixed bed column will be optimised using the ground-breaking analysis.

Additionally, a variety of factors, such as flow velocity, size of the sorbent, sorbate concentration, isotherm type, temperature, pH, and others, affect each FBR system's breakpoint appearance. The kinetic energy of molecules rises with temperature due to the random motion of molecules in fluids and the increase in vibrations in solids. The random movement of molecules in fluids and the increase in vibrations in solids cause the kinetic energy of molecules to increase with temperature. This could result in increased collisions between the substances molecules and other surfaces. This can lead to more interactions between the molecules of the drug and other surfaces.

For precise flow rate selection in several FBR experiments, effluent flow data for betel seeds of various diameters with a depth of 30 cm were employed. The fixed beds' apparent or actual radial biosorption is improved by flow across the porous bed. Plastic pipe media will enhance the porosity of the media in the reactor by increasing the adsorbent's ability to cling to it.

The observed effluent flows ranged from 91 to 218 millilitres per minute (for 0.32 mm size) and from 221 to 324 millilitres per minute (for 0.32 mm size) (for 0.6 mm size). An appropriate movement rate of 60 ml/min was established for the sorption of Cr (IV+) by varied sizes in FBR because the discharge flow rate was sharp even at a 30 cm depth of the size of the sorbent (0.13 mm). Biosorption capacity is related to concentration of sorbate on the sorbate surface, and the efficiency determines progress of biosorption process. The higher the biosorption capacity of the sorbent, the higher its efficiency for removing pollutants

3. Result and discussion

3.1. Removal of Cr (VI^{+}) using fixed bed column

The right concentrations of Cr (VI+) effluents were synthesised. Four columns with diameters of 5 cm and heights of 100 cm were employed in a laboratory setting for column operation. The formula below is used to determine the heavy metal's capability for biosorption;

$q= (Ci-Ce/m) * v,$

where Ci= initial concentration Ce= concentration at equilibrium (mg/L), v=volume (L), m= mass (g)

A sand filter was positioned at the bottom of the column before charging the material in the bed, and the packing material was charged above it (Balaji *et al*., 2022). Langmuir, Yoon-Nelson, (BDST), Thomas, Elovich equation, the pseudo-first-order equation, and the pseudo-second-order equation are a few that are used to support their findings models. Kinetic modelling is a technique that may be utilised while evaluating novel adsorbents. Sips, Dubinin raduskevich, and Freundlich may all be utilised for equilibrium modelling.

Gravity was used to let the sewage flow through the bed. The flow was controlled by a needle valve. At the bottom, a collection of the treated effluent was made for analysis.

3.2. Bed enactment with a diverse initial concentration

In Figure 1, it was shown that the contact time (at 1.7% saturation level) is inversely related to the initial Cr (VI+) concentration. The biosorptive capacity (from service length and beginning Cr (VI+) concentration) fluctuates, as demonstrated by the graph. As the starting Cr (VI+) concentration increased (Figure 1), the service duration was shortened, and as a result, the biosorptive capacity increased linearly. This may be explained by the governing mass-exchange condition, which stipulates that the focus slope, the area opposing the mass transition, and the mass-transfer coefficient all affect the mass-transfer motion. The sorption isotherm's form describes the affinity of the sorbate for the adsorbent and sheds light on potential interactional mechanisms. The categorization for liquid-solid adsorption systems allows for the classification of both observable isotherms as L curves. The depth parameters determine how well impurities are removed from the reactor, therefore as the depth of the reactor increases, so does the removal efficiency of heavy metal concentration, or vice versa.

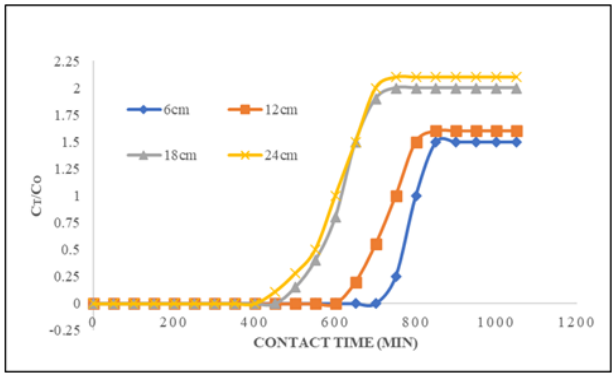


Figure 1. Performance of BED column for different initial - concentrations of Cr^{6+}

A larger attention tendency is correlated with greater initial fixation. As a result, this important mass exchange driving force causes bed limit to advance more quickly than bed administration time. Additionally, a relationship

between Cr (VI+) starting concentration (C0) and biosorptive capacity (N0) was found and is shown in Eq. 1.

$$N_o = 0.09\, C_o \quad (1)$$

3.3. Bed performance with particle size

In an FBR operation, the biosorbent size significantly affects the bed porosity as well as the flow rate. As can be shown, the amenity time (at 1.8% capacity) decreases as the geometric mean particle size rises (Reynolds *et al*., 1996). Because the experimental Reynolds number (Re) varied between 0.41 and 1.29 (with Wadell constant, = 0.7, = 985 kg/m3, v = 1.15x10-3 m/s, particle sizes 0.32, 0.6, and 1 mm, and = 0.113x10-3 Ns/2) the Wilson and Geankoplis correlation model (for Re between 0.0026 and 65) can be used to explain the effect of particle size on Cr (VI+) removal in FBR. According to the model,

$$J_d = \left(1.09 x R_e^{-2/3}\right) / €\quad (2)$$

Where J_d is the dimensionless mass-transfer factor and € is either the bed void fraction or bed porosity (dimensionless). Jd values from Equation 2 range from 2.12 (for a size of 0.32 mm) to 0.941 (for a size of 1 mm). Typically, batch tests will be utilised to identify the starting doses. In some circumstances, the concentration of the raw effluents will be taken into account to determine the best value. Controlling the temperature of the feed and the column bed with a small scale column and a water bath, heating tapes with regulators wrapped around the column can also be used to adjust the temperature. The relevant Jd values will somewhat rise as the bed porosity drops with a reduction in betel seed size, increasing the bed capacity of the betel seeds, even if the actual bed porosity was not available or evaluated.

3.4. Bed performance with flow rate on breakthrough curves

An unsteady-state condition develops when a solution is passed through a stationary sorber because the sorbent continuously absorbs more and more sorbate. The easiest method is to divide the volumetric flow rate (m^3/min) by the fixed bed's cross-sectional area (m^2). The sorption zone that is in equilibrium with the influent concentration moves downward as the solution flows downhill through the bed, continuing the flow. Figures 2–4 show that the period for BSP breakthrough and fatigue reduces with flow rate. As shown in Figures 2–4, the breakthrough point was achieved at flow rates of 40, 60, and 100 ml/min in 75, 68, and 54 minutes, respectively. The times to exhaustion were, respectively, 270, 220, and 280 minutes. An essential aspect of column operation and design in FBR research is the evaluation of the breakthrough curve, which is the plot of fractional sorbate concentration at any time t with regard to C0 vs. service time or contact time t.

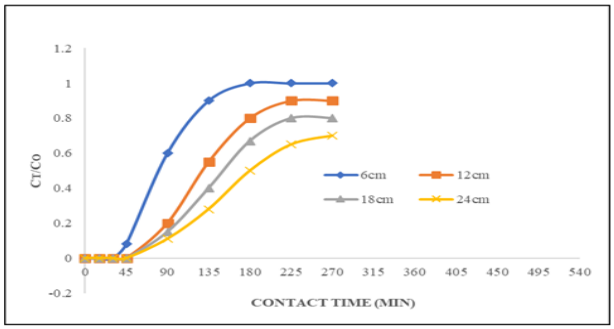


Figure 2. Breakthrough curves for diverse bed depths-40ml/min movement rate

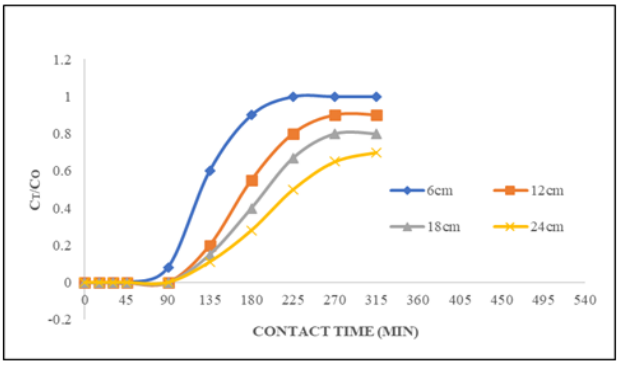


Figure 3. Breakthrough curves for changed bed depths-60ml/min movement rate

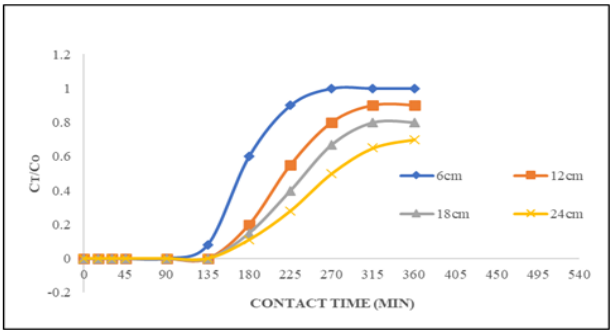


Figure 4. Breakthrough curves for various bed depths at a flow rate of 100 ml/min

3.5. Performance with bed height on Breakthrough Curves:

In order to assess column performance, the bed height was changed between 6 and 42 cm while maintaining a constant flow rate and starting concentration. Calculating the breakthrough time requires the breakthrough curve to be present. In order to do this, we can run a column with any diameter and length to determine the real capacity and length of the equilibrium section. The diameter and length can be recalculated using those factors. The breakthrough curves at various bed height values are shown in Figure 5. Higher BDST values and bed heights were shown to enhance equilibrium capacity, removal percentage, and effluent volume. Figure 6 displays the effectiveness of the removal % of Cr^{6+} ions.

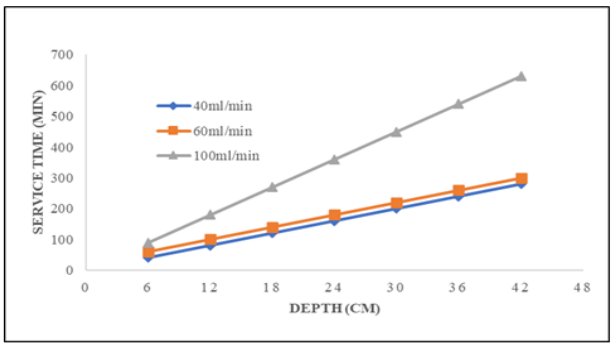


Figure 5. Bed depth Vs service time

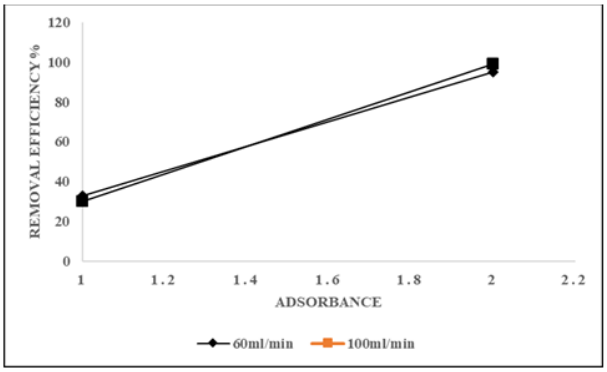


Figure 6. Overall Efficiency vs Absorbance

4. Conclusion

In a continuous experiment, as the bed height rose from 2.2 to 6.5 cm, the removal % and time to breakthrough increased; the greatest adsorption capacity was attained at 6.5 cm. When the flow rate was decreased from 100 to 40 mL/min, it took longer to reach the breakthrough; however, this time could be cut in half by increasing the concentration of the Cr (VI^+) solution at the input. The biosorption model's strong match to the BDST was confirmed by the experimental data. The behaviour of Cr (VI^+) biosorption in a continuous fixed-bed column system containing Cr (VI^+) may thus be assessed using a model of this kind. During four cycles of regeneration research, it is necessary to investigate the operation and the dynamic response of the system in order to determine the breakthrough curve of each metal. The amount of biosorption was detected in subsequent cycles, revealing the distinct potential for re-utilization.

References

Arivoli S., Marimuthu V., Ravichandran T. and Hema Kinetic M. (2012). Equilibrium and Mechanistic Studies of Nickel Adsorption on A Low Cost Activated Calcite Powder *Indian Journal of Science and Technology*, **1**(1), 41−49

Arumugam T., Kinattinkara S., Kannithottathil S., Velusamy S., Krishna M. and Sivakumar V. (2022). Comparative assessment of groundwater quality indices of Kannur District, Kerala, India using multivariate statistical approaches and GIS, *Environmental Monitoring and Assessment*, **29**

Bailey S.E., Olin T.J., Bricka R.M., Adrian D. (1999). A review of potentially low-cost sorbents for heavy metals. *Water Research* **33** (11), 2469–2479.

Balaji G., Rajan M.S., Kumar G.R., Vivek S. and Gokulan. (2022). Biosorption of chromium (VI+) using tamarind fruit shells in continuously mixed batch reactor 25, Rgnest_04561. https://doi.org/10.30955/gnj.004561

Blanco C., Santamarı R., Botas C., Patricia A., Rodrı F., Granda M. *et al*. (2012). Critical temperatures in the synthesis of graphene-like materials by thermal exfoliation – reduction of graphite oxide, Carbon N Y, **2,** 476–85

Cabatingan L.K., Agapay R.C., Rakers J.L.L., Uttens M. and Weilen L.A.M. (2001). Potential of Biosorption for the Recovery of Chromate in Industrial Wastewaters, *Industrial & Engineering Chemistry Research*, **40,** 2302−2309

Chan S.S., Chow H. and Wong M.H. (1991). Microalge as a bioabsorbents for treating mixture of electroplating and sewage effluent, *Biomedical and Environmental Sciences,* **4** 250–260

Chanda M. and Rempel G.L. (1993). Selective Chromate Recovery with Quartermized Poly (4-Vinylpyradine), *React Polymer*, **21**, 77.

Dabrowski A., Hubicki Z., Podkoscielny P. and Robens E. (2004). Selective removal of the heavy metal ions from waters and industrial wastewaters by ion-exchange method, *Chemosphere*, **56**, 91–106.

Demiral P. and Gunduzoglu G. (2010). Removal of nitrate from aqueous solutions by activated carbon prepared from sugar beet bagasse, *Bioresource Technology*, **101** 1675–1680.

Ganapathy G.P., Alagu A., Ramachandran S., Panneerselvam A.S., Arokiaraj G.G.V., Panneerselvam M., Panneerselvam B., Sivakumar V. and Bidorn B. (2023). Effects of fly ash and silica fume on alkalinity, strength and planting characteristics of vegetation porous concrete, *Journal of Materials research and technology*, **24**, 5347−5360

Ghosh S., Sarkar A. and Nayek H.P. (2021). Elucidation of selective adsorption study of Congo red using new Cadmium (II) metal-organic frameworks: Adsorption kinetics, isotherm and thermodynamics, *Journal of Solid-State Chemistry*, **296**, 121929

Gokulan R., Kalyani G. and Killi S. (2022). Removal of Reactive Red 120 in a Batch Technique Using Seaweed-Based Biochar: A Response Surface Methodology Approach, *Journal of Nanomaterials, Hindawi Publications*, Article ID 7604383, https://doi.org/10.1155/2022/3621807, (Indexed in SCI I.F: 3.79, Q2)

Gokulan R., Pradeepkumar S. and Elias G. (2021). Continuous Sorption of Remazol Brilliant Orange 3R Using Caulerpa scalpelliformis Biochar, *Advances in Materials Science and Engineering*, Article ID 6397137, 7

Hariprasad C.P. and Geresh M. (2009). Biosorption of Malachite Green from Aqueous Phase by CMBR and FBR, Proc. of National Conf on Innovations in Civil Engg, ICE 09.

Hell F., Lahnsteiner J., Frischherz H. and Baumgartner G. (1998). Experience with Full Scale Electrodialysis for Nitrate and Hardness Removal, *Desalination* **117**, 173.

Huang and Ostovic. (1978). Removal of Cadmium (II) by Activated Carbon Adsorption, *American Society of Civil Engineers*, **104** (5).

Hui K.S., Chao C.Y.H. and Kot S.C. (2005). Removal of mixed heavy metal ions in wastewater by zeolite 4A and residual products from recycled coal fly ash, *Journal of hazardous materials,* **127** 89–101.

Jegan J., Praveen S., Pushpa T.B. and Gokulan R. (2020). Sorption kinetics and isotherm studies of cationic dyes by arachis hypogaea shell derived biochar as low-cost adsorbent, *Applied Ecology and Environmental Research*, **18** (1), 1925−1939.

Khan A.A. and Singh R.P. (1987). Adsorption Thermodynamic of Carbon furan on Sn(IV) Arsenosilicate in H+, Na+, and Ca2+ forms, *Colloids and Surfaces*, **24**, 33−42

Kinattinkara S., Arumugam T., Samiappan N. and Sivakumar V. (2022). Deriving an Alternative Energy Using Anaerobic Co-Digestion of Water Hyacinth, *Food Waste and Cow Manure, JREE*

Kumar M., Sujatha S., Gokulan R., Vijayakumar A., Praveen S. and Elayaraja S. (2021). Prediction of RSM and ANN in the remediation of Remazol Brilliant Orange 3R using biochar derived from Ulva Lactuca, *Desalination and Water Treatment*, **211**, 304−31

Lenin Sundar M., Kalyani G., Gokulan R., Ragunath S. and Joga Rao H. (2021). Comparative adsorptive removal of Reactive Red 120 using RSM and ANFIS models in batch and packed bed column, *Biomass Conversion and Biorefinery*.1−17

Lin S.H., Lai S.L. and Leu H.G. (2000). Removal of heavy metals from aqueous solution by chelating resin in a multistage adsorption process, *Journal of hazardous materials,* **76** 139–153

Mani S., Murugesan S.R., Ganesan R. and Sivakumar V. (2022). Biosorption of Nitrate by Thermodynamic and Kinetics study using Tamarind Fruit Shells, *Global NEST Journal*, **24**(4), 720−728; https://doi.org/10.30955/gnj.004480

Murugadoss J.R., Balasubramaniam N., Gokulan R., Rajesh G.N.K., Sreelal P., Sudam A.P., Rahman Z.D.R. and Ali R.N.(2022). Optimization of River Sand with Spent Garnet Sand in Concrete Using RSM and R Programming Packages, *Journal of Nano Materials, Hindawi Publications*, Article ID 4620687

Murugesan S.R., Ganesan R., Vivek Sivakumar Mani S. (2022). Biosorption of Nitrate by Thermodynamic and Kinetics study using Tamarind Fruit Shells, *Global Nest Journal*, **24**

Murugesan S.R., Sivakumar V. and Panneerselvam M. (2022). Biosorption of Malachite Green from Aqueous Phase by Tamarind Fruit Shells Using FBR, *Advances in Materials Science and Engineering*.

Murugesan S.R., Sivakumar V., Velusamy S., Ravindiran G., Sundararaj P., Maruthasalam V., Thangavel R., Ramasamy G.S., Panneerselvam M. and Periyasamy S. (2022). Biosorption of Malachite Green from Aqueous Phase by Tamarind Fruit Shells Using FBR, *Advances in Material Science and Engineering*, Article ID 8565524 | https://doi.org/10.1155/2022/8565524

Periyasamy S., Murugesan R.S., Sivakumar V., Velusamy S. and Ravindiran G. (2022). Biosorption of Malachite Green from Aqueous Phase by Tamarind Fruit Shells Using FBR, 8565524, *Advances in Materials Science and Engineering*

Peters R.W., Young K. and Bhattacharyya D. (1985). Evaluation of recent treatment techniques for removal of heavy metals from industrial wastewaters. *AICHE Symp. Series* **81**, 160−1703.

Rajan M.S., Kumar G.R., Vivek S., Gokulan R. and Balaji G. (2022). Biosorption of chromium (VI+) using tamarind fruit shells in continuously mixed batch reactor, *Global NEST Journal*, **25**, No 1, 180−186.

Ravindiran G., Elayaraja S., Navaneethan P., Rajeshkannan R. and Abinaya S. (2014). Assessment of physicochemical characteristics of municipal wastewater by microalgae *International Journal of ChemTech Research*, **06** (01), 515-520

Rengaraj S., Kyeong-Ho Y. and Seung-Hyeon M. (2001). Removal of chromium from water and wastewater by ion exchange resins, *Journal of hazardous materials,* **87,** 273– 287.

Reynolds T.D. and Richards P.A. (1996). Unit Operations and Processes in Environmental Engineering, 2nd edition. PWS, Boston U.S.A

Sampranpiboon P. and Charnkeitkong P. (2010). Equilibrium Isotherm, Thermodynamic and Kinetic Studies of Lead adsorption onto pineapple and paper waste sludges, *International Journal of Energy and Environment*, **3**(4)

Sivakumar V., Sashik kumar M.C. and Natarajan L. (2022). Vulnerability Assessment of Groundwater in Industrialized Tiruppur Area of South India using GIS-based DRASTIC model, *Journal of Geological Society of India*, **98**

Spinti M., Zhuang H. and Rujillo E.M. (1995). Evaluation of immobilized biomass beads for removing heavy metals from wastewater. *Water Environment Research*. **67**, 943−952

Sundar M.L., Ragunath S., Hemalatha J. and Vivek S. (2022). Simulation of ground water quality for noyyal river basin of Coimbatore city, Tamilnadu using MODFLOW, Chemosphere, 306, 135649

Sundaramoorthy D., Subramanian K., Tanneeru M., Govindasamy R. and Vivek S. (2022). Block-level Drought Assessment using Rainfall and Remote sensing Data 24 gnest_04485

Thirukumaran T., Krishnapriya S., Priya V., Britto S.F., Anandhalakshmi R., Dinesh S., Poomalai R., Vivek S. and Saravanan S. Utilizing rice husk ash as a bio-waste material in geopolymer composites with aluminium oxide, *Global NEST Journal*, https://doi.org/10.30955/gnj.004694

U. Forstner G.T.W. (1979). Wittman, Metal Pollution in Aquatic Environment, Springer Verlag, Berlin

Vignesh S.R. Vivek V., Priya K. and Thanukrishna. (2020). Experimental Investigation on Bricks by Using Cow Dung, *Rice Husk, Egg Shell Powder as a Partial Replacement for Fly Ash* **9**

Wales D.S. and Sagar B.F. (1990) Recovery of metal ions by microfungal ®lters. *Journal of Chemical Technology and Biotechnology,* **49**, 345−355.

Xiong M., Yang M., Chen Q. and Cai T. (2022). Mechanism studies for adsorption and extraction of soluble sodium from bauxite residue: Characterization, kinetics, and thermodynamics, *Chemical Engineering* **10**(4), 108183